Mathematical Biosciences and Engineering

https://www.aimspress.com/journal/mbe

MBE, 23(4): 1096–1120.
DOI: 10.3934/mbe.2026041
Received: 15 January 2026
Revised: 17 February 2026
Accepted: 26 February 2026
Published: 10 March 2026

Research article

Modelling infectious disease transmission dynamics in conference environments: An agent-based approach

Xue Liu[1,2,†], Yue Deng[3,†], Jingying Huang[4,5], Yuhong Zhang[3] and Jinzhi Lei[1,4,*]

[1] School of Mathematical Sciences, Tiangong University, Tianjin 300387, China
[2] School of Mathematics, Shandong University, China
[3] School of Software, Tiangong University, Tianjin 300387, China
[4] School of Computer Science and Technology, Tiangong University, Tianjin 300387, China
[5] Shanghai Qinhe Web Technology Software Development Co., Ltd
[6] Center for Applied Mathematics, Tiangong University, Tianjin 300387, China
[†] These authors contributed equally.

[*] **Correspondence:** Email: jzlei@tiangong.edu.cn.

Abstract: The looming threat of infectious diseases perpetually challenges the global public health landscape. Central to addressing this concern is the imperative to prevent and manage disease transmission during pandemics, particularly in unique settings. This study addresses the transmission dynamics of infectious diseases within conference venues by presenting a computational model that simulates transmission processes over a condensed timeframe (one day), beginning with sporadic cases. Our model captures the activities of individual attendees within the conference venue, including meetings, rest breaks, and meal breaks. While meetings entail proximity seating, rest and lunch periods allow attendees to interact with diverse individuals. Moreover, the restroom environment poses an additional avenue for potential infection transmission. Employing an agent-based model, we meticulously replicated the transmission dynamics of infectious diseases, with a specific emphasis on close-contact interactions between infected and susceptible individuals. Through comprehensive analysis of model simulations, we elucidated the intricacies of disease transmission dynamics within conference settings and assessed the efficacy of control strategies to curb disease dissemination. Ultimately, our study provides a numerical framework for assessing the risk of infectious disease transmission during short-duration conferences, furnishing conference organizers with valuable insights to inform the implementation of targeted prevention and control measures.

Keywords: COVID-19; infectious disease; agent-based model; computational model; epidemic dynamics

1. Introduction

The profound impact of the COVID-19 pandemic on global public health and economic stability over the past few years underscores the critical need for comprehensive reflection on preventive measures and disease control strategies [1, 2]. As the pandemic era wanes, we must scrutinize and enhance our understanding of measures to curb the spread of infectious diseases. Despite the extensive body of literature on epidemic dynamics and forecasting, there remains a paucity of research on disease transmission dynamics within specific contexts. Notably, evaluating the potential for disease outbreaks following large-scale international events, such as conferences and business meetings, is paramount in an era of interconnectedness and globalization.

Numerous mathematical models have been proposed to predict the dynamics of epidemics and to evaluate the efficacy of various prevention and control strategies. These models often take the form of differential equations based on the SIR (susceptible-infectious-recovered) or SEIR (susceptible-exposed-infectious-recovered) frameworks [3–7]. Additionally, data-driven models have emerged to forecast dynamics by analyzing reported data [8–11]. While compartmental and data-driven models are valuable for examining community transmission during epidemics, they may not adequately capture sporadic transmission within specific settings.

To address the stochastic dynamics of disease transmission arising from close interpersonal contact, researchers often employ agent-based models, which simulate the epidemic progression for each individual [12–15]. Recent advances in agent-based modeling have extensively explored transmission dynamics in structured environments. For instance, [16, 17] have successfully modeled COVID-19 spread in education settings, emphasizing the role of classroom cohorts. Similarly, [18, 19] have focused on workplaces and public transport, utilizing empirical contact matrices to estimate infection risks. Many other agent-based models have also been developed to simulate the transmission dynamics of infectious diseases by focusing on individual mobility, crowd dynamics, close contact between individuals, and heterogeneous responses among individuals [20–24].

However, academic and professional conferences represent a distinct epidemiological niche that remains under-explored. Unlike schools (routine interactions) or unstructured crowds (random mixing), conferences function as hybrid systems: they oscillate between highly structured, static phases (lecture sessions) and unstructured, high-density mixing phases (coffee breaks, lunches). Crucially, the rigid scheduling of conferences creates synchronized movements, leading to severe spatiotemporal bottlenecks—such as overcrowding in restrooms or buffet lines within short time windows. Existing general-purpose models often simplify these granular dynamics into average contact rates, potentially underestimating the risk at these specific hotspots.

To address this gap, we propose a specialized agent-based framework designed explicitly for the conference ecosystem. Our model integrates detailed module constraints—tracking the transition from fixed seating to random mixing and queuing—to quantify the impact of specific logistical interventions (e.g., changing lunch layouts or staggering restroom breaks) that general models cannot easily assess.

The present study aims to develop a computational model capable of simulating the spread of infectious diseases within the confines of a one-day conference venue, with a specific focus on respiratory diseases caused by viral infections. Our model incorporates various activities—such as meetings, breaks, and meal times—that participants typically engage in, facilitating dynamic contact patterns as individuals interact with diverse attendees throughout the day. Moreover, we acknowledge

the potential for infection transmission in restroom facilities due to environmental factors. The agent-based model proposed in this study offers a quantitative approach to assessing the risk of disease transmission during short-duration conferences and evaluating diverse prevention and control strategies to mitigate the spread of infection.

2. Materials and methods

2.1. Agent-based model

We investigated the dynamics of a one-day conference involving N participants, denoted as C_i, where i ranges from 1 to N. Initially, only a handful of participants were assumed to be infected with the virus prior to the conference. Our analysis was confined to activities within the conference venue, as depicted in Figure 1(a). Transmission events may arise from interpersonal infections or environmental contamination in restroom facilities. To simulate disease spread, we employed an agent-based model formulated in continuous time—capturing the instantaneous nature of transmission—and implemented it numerically using a discrete time step Δt.

In our model, each of the N individuals is characterized by their epidemic status, classified as susceptible (S), exposed (E), or infectious (I). At the outset, all individuals are either susceptible or infectious, with susceptibility transitioning to exposure upon contact with the virus during the conference. Given the duration of a one-day conference, individuals typically do not progress from exposure to infectiousness within the same day. We adopted an SEI model to delineate the progression of epidemic statuses, whereby the infectious compartment remains stable throughout the conference duration (Figure 1(b)).

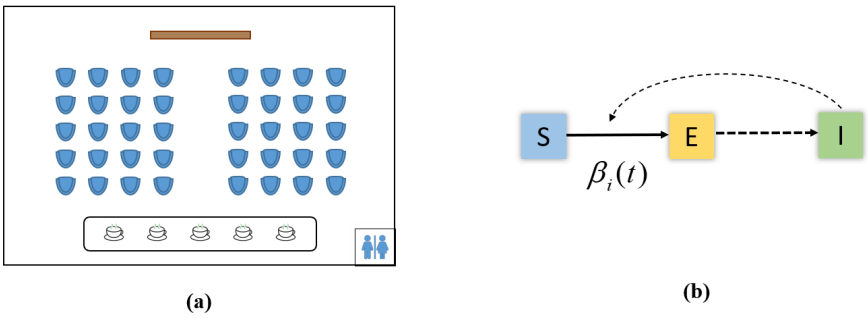

Figure 1. (a) Status map of the conference venue. (b) Schematic representation of the agent-based model illustrating disease transmission dynamics and the SEI model for each individual. Individuals transition among the susceptible (S), exposed (E), and infectious (I) states as indicated by the arrows. Transition rates are individual-dependent and may vary over time.

Our model intricately captures each participant's activities as outlined in the conference itinerary, including meetings, breaks, and meals. The daily itinerary detailed in Table 1 serves as a representative scenario to initialize the temporal contact dynamics in our simulation. During meetings, participants remain stationary, whereas during breaks and meal times, they can move about and engage with others. Notably, restroom visits during these intervals pose a potential risk of infection transmission. By

simulating these individual activities, we estimated the potential number of individuals susceptible to infection following a one-day conference.

It is important to note that the schedule in Table 1 acts as a generic input parameter for illustrative purposes and does not reflect the specific practices of any particular region. The proposed agent-based model is designed with intrinsic flexibility, allowing the time-dependent contact matrices to be recalibrated to fit any arbitrary conference schedule or logistical arrangement.

Table 1. The schedule of the conference.

8 : 30 – 9 : 00	Rest time
9 : 00 – 10 : 00	Meeting
10 : 00 – 10 : 30	Rest time
10 : 30 – 12 : 00	Meeting
12 : 00 – 14 : 00	Lunch break
14 : 00 – 16 : 00	Meeting

2.2. Individual activities

We analyzed each individual C_i, considering their spatial dynamics, represented by $\vec{r}_i$, and their epidemic status, denoted as s_i. The epidemic status is classified as susceptible (S), exposed (E), or infectious (I), with the transition from susceptible to exposed occurring subsequent to an infection event (to be detailed below).

To capture the movement of individuals across different locations $\vec{r}_i(t) = (x_i(t), y_i(t))$, we delineated two distinct modes: meeting and resting. During the meeting, participants are seated and stationary, adhering to the pre-arranged seating arrangements. Typically, participants are assigned fixed seats for the duration of the conference. When seat assignments vary, participants generally return to their original seats after breaks. Hence, we assumed each participant occupies a designated seat during the meeting sessions.

Conversely, during resting periods or the lunch break, participants can vacate their seats, traverse the venue, and engage in conversations. Movement patterns are simulated using a numerical two-dimensional random walk scheme, with parameters detailed in Table A1 in Appendix A. Moreover, when individuals come into close proximity, they may pause briefly to engage in conversation before resuming their walk. Restroom visits were also accounted for during resting periods or the lunch break. Furthermore, participants may opt to remove their masks during the lunch break, thereby significantly reducing the mask-wearing rate. After the resting or lunch break period, most participants return to their original positions; however, a small fraction of participants, say 10%, may change their seats.

2.3. Restroom timing

Restrooms are high-risk areas for the transmission of infections within the conference venue. To accurately model infection events in these areas, it is crucial to estimate the stochastic timing of participants' restroom visits. While the interval between restroom visits for an individual typically follows an exponential distribution, participants generally avoid visits during meeting sessions. Consequently, the timing estimation must be adjusted to align with the conference schedule constraints.

To determine the timing of the next restroom visit, we calculate the probability density of a participant visiting the restroom at a delay a from the current time t. Let $p(a;t)$ be the probability density function such that $p(a;t)\Delta a$ denotes the probability that a participant will use the restroom during the time interval $(t+a, t+a+\Delta a)$, measured from the current time t.

We introduce two-component functions to construct $p(a;t)$. Let $f(a;t)$ denote the baseline density function derived from the physiological urge, such that $f(a;t)\Delta a$ indicates the intrinsic probability of a visit. Additionally, let $q(a;t)$ represent that schedule availability function (or the complement of the refraining probability), which acts as a weighting factor based on the conference itinerary (e.g., q is low during meetings and high during breaks). Based on $f(a;t)$ and $q(a;t)$, the conditional probability density $p(a;t)$ is formulated as:

$$\begin{aligned} p(a;t) &= C(t)^{-1} f(a;t) q(a;t), \\ C(t) &= \int_0^{+\infty} f(a;t) q(a;t) \mathrm{d}a, \end{aligned} \tag{2.1}$$

where $C(t)$ serves as the normalization constant. Detailed derivations of the functions $q(a;t)$, $f(a;t)$, and $p(a;t)$ are provided in Appendix B.

To determine the specific waiting time a until the next visit, we utilize the cumulative distribution function $F(a;t)$, defined as:

$$F(a;t) = \int_0^a p(a';t)\mathrm{d}a'.$$

By employing the inverse transform sampling method with a uniform random number $s \in [0,1]$, we solve the equation $s = F(a;t)$ to find the waiting time a. The next restroom visit is effectively scheduled at time $t+a$. The detailed numerical scheme for this procedure is outlined in Appendix B.

Utilizing this scheme, we assume that at the beginning of the simulation (or after each visit), the time for the next restroom visit is generated for each participant according to their schedule $\{T_i\}$. Once a participant enters the restroom, the duration of stay is determined by a random number generated from a Gamma distribution. Upon completion of the visit, the next scheduled visit time is recalculated, and the process repeats.

2.4. Virus transmission

We investigated two scenarios of virus transmission: direct transmission from an infectious individual to a susceptible individual through close contact, and indirect transmission via a contaminated restroom environment.

2.4.1. Close contact infection

Participants' movement primarily occurs during rest or lunch breaks. Two individuals are considered in close contact if their spatial distance is within a threshold, denoted the close contact distance (*cdm*). Furthermore, close contact may occur during meetings if the distance between adjacent seats is less than cdm. For individuals i and j in close contact, the cumulative interaction duration is denoted as $t_{i,j}$. When a susceptible individual encounters an infectious individual, the likelihood of exposure depends on the duration of contact and the specific transmission-prevention measures in place.

Let $\beta_{\max}$ denote the maximum transmission probability when a susceptible individual comes into contact with an infectious individual for a sufficiently long duration. The infection probability of a susceptible individual i by an infectious individual j over a contact duration $t_{i,j}$ is modeled as:

$$\beta_{i,j}(t_{i,j}) = \beta_{\max} \times (1 - e^{-t_{i,j}/\tau}) \times M_{i,j}. \tag{2.2}$$

Here, τ represents the characteristic time constant governing the saturation of infection risk, and $t_{i,j}$ indicates the specific contact duration. The term $M_{i,j}$ represents the attenuation factor characterizing the protective barrier of face masks. Consistent with empirical estimates and clinical observations [25–28], we define $M_{i,j}$ for four distinct scenarios:

$$M_{i,j} = \begin{cases} 1.0, & \text{if both } i \text{ and } j \text{ are unmasked,} \\ 0.33, & \text{if } i \text{ is masked and } j \text{ is unmasked,} \\ 0.11, & \text{if } i \text{ is unmasked and } j \text{ is masked,} \\ 0.017, & \text{if both } i \text{ and } j \text{ are masked.} \end{cases} \tag{2.3}$$

These values reflect the asymmetric nature of mask protection. The value 0.33 corresponds to a 67% reduction in susceptibility for the wearer, while 0.11 represents a more potent source control efficiency (89%) in blocking the shedding of infectious droplets at the origin [27, 28]. Notably, the factor 0.017 for the dual-masking scenario is lower than the simple product of independent probabilities ($0.33 \times 0.11 \propto 0.036$). This choice accounts for the synergistic effect of universal masking: beyond additive filtration, a significant reduction in the velocity and concentration of the initial exhaled plume from the source further enhances the filtration efficiency for the susceptible individual [25, 28].

To incorporate the effect of vaccine protection, let V_i represent the protective efficacy of vaccination (or immunity from prior infection) for individual i. When a susceptible person i is in contact with multiple infectious individuals, the aggregate infection probability β_i is given by

$$\beta_i = \left(1 - \prod_{j \text{ contacts with } i} (1 - \beta_{i,j}(t_{i,j}))\right) \times (1 - V_i), \tag{2.4}$$

where we set

$$V_i = \begin{cases} 0, & \text{if } i \text{ is not vaccinated} \\ 0.3, & \text{if } i \text{ is vaccinated or recovered} \end{cases} \tag{2.5}$$

in our model simulation.

2.4.2. Infection from the contaminated restroom

To quantify the infection risk in the restroom, we model temporal changes in virus concentration and estimate the transmission rate from the contaminated environment to individuals.

In the restroom, virus concentration increases due to exhalations from infectious individuals and decreases through ventilation or disinfection. Assuming each infectious individual releases the virus at a rate α and the virus is diluted at a time-dependent rate $b(t)$, the concentration $X(t)$ evolves according to

$$\frac{\mathrm{d}X}{\mathrm{d}t} = \frac{1}{V} \sum_{\text{infections } i} \alpha G_i \varepsilon_i(t) - b(t)X(t), \tag{2.6}$$

where V is the restroom volume, and $\varepsilon_i(t)$ is an indicator function:

$$\varepsilon_i(t) = \begin{cases} 1, & \text{if } i \text{ is in the restroom,} \\ 0, & \text{otherwise.} \end{cases} \tag{2.7}$$

The factor G_i quantifies the reduction in viral shedding by infectious individual i due to mask-wearing, defined as:

$$G_i = \begin{cases} 1, & \text{if } i \text{ is unmasked,} \\ 0.11, & \text{if } i \text{ is masked.} \end{cases} \tag{2.8}$$

When a susceptible individual enters the restroom, the risk of infection depends on the current viral concentration and their own mask-wearing status, K_i:

$$K_i = \begin{cases} 1, & \text{if } i \text{ is unmasked,} \\ 0.33, & \text{if } i \text{ is masked.} \end{cases} \tag{2.9}$$

The infection rate is modeled using a Hill-like function to represent the saturation effect of virus concentration:

$$\beta_i(t) = \beta_{\max} \frac{(X(t)/X_0)^4}{1 + (X(t)/X_0)^4} K_i(1 - V_i), \tag{2.10}$$

where X_0 denotes the reference virus concentration.

Furthermore, we consider environmental contamination through surface contact (e.g., door handles, toilet seats, and sinks). The probability of infection after using the restroom also depends on interactions with these objects and hand hygiene practices. The comprehensive probability of infection via this route for individual i is denoted as $\mu_i(t_0, s)$; see Appendix C for the detailed derivation.

Integrating both aerosol and surface routes, the total likelihood of infection for an individual using the restroom from $t = t_0$ and $t = t_0 + s$ is

$$p_i(t_0, s) = 1 - \left[\exp\left(- \int_{t_0}^{t_0+z} \beta_i(s) \mathrm{d}z \right) \times (1 - \mu_i(t_0, s)) \right]. \tag{2.11}$$

Detailed derivations are provided in Appendix D.

For our simulations, we focus on highly transmissible variants such as SARS-CoV-2 Omicron, assuming a maximum transmission infected probability $\beta_{\max} = 0.9$ [29, 30]. Moreover, the choice of Δt is set to be sufficiently small (e.g., 1 second) such that the probability of multiple events occurring within a single interval is negligible, thereby maintaining the fidelity of the continuous-time underlying process.

3. Results

We employed the agent-based model to analyze disease transmission dynamics during a one-day conference. Our objective was to assess the extent of infections among participants following the event, starting with a small number of initially infected individuals. For the simulations, we utilized the schedule outlined in Table 1, with the conference commencing at 9:00 am and all participants arriving 30 minutes prior. Unless otherwise stated, all simulations described below considered a scenario with $N = 250$ participants and 3 initially infectious individuals.

3.1. Infections without control measures

Initially, we explored scenarios in which no control measures—such as mask-wearing, vaccination, or restroom ventilation—were implemented. Our simulations estimated the cumulative number of infections by the end of the one-day conference. In the absence of intervention, the simulations revealed that the number of infections ranged from 100 to 240, corresponding to a mean attack rate of approximately 84%.

Although this attack rate appears substantial, it is consistent with empirical observations from documented super-spreading events in confined indoor environments. For instance, the Skagit Valley Choir outbreak recorded an attack rate of 86.7% in the absence of interventions [31], and the Omicron outbreak at a Christmas party in Oslo resulted in a 74% infection rate despite high vaccination coverage among participants [32]. These real-world cases corroborate the plausibility of our simulation results under high-density, uncontrolled conditions. Figure 2(a) illustrates the frequency distribution of the total number of infections.

To further investigate the infection dynamics, we examined the average infection counts during distinct phases of the event, including resting periods, meetings, lunch breaks, and restroom use (Figure 2(b)). Our analyses revealed that fewer infections occurred during meetings, whereas most transmission events occurred during lunch breaks and rest periods. Notably, a significant number of infections were also attributed to restroom usage. Furthermore, our results indicate that the ratio of infections caused by aerosol inhalation to those caused by surface contact was approximately 5:1. This disparity underscores the critical role of ventilation in controlling the spread of infection. These findings highlight the need to implement control measures during unstructured breaks and to prioritize interventions such as restroom ventilation to mitigate transmission risk.

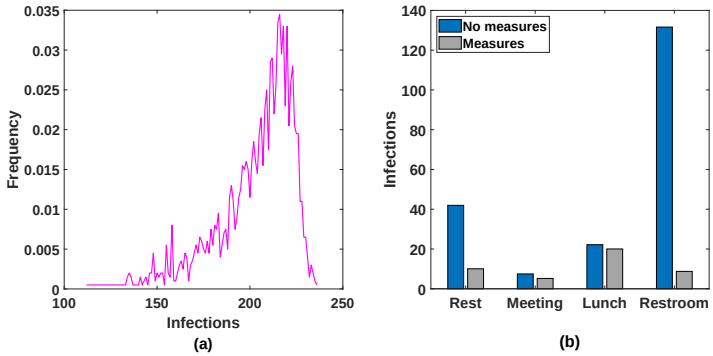

Figure 2. Comparison of infection numbers with and without prevention and control measures. (a) Distribution of cumulative infections without prevention and control measures. The horizontal axis represents the number of infections, while the vertical axis denotes the frequency of occurrence. (b) Distribution of infections across various activities. Color bars indicate the average number of infections during resting, meetings, lunch breaks, and restroom usage, with or without prevention and control measures. All results were derived from 2000 independent runs.

3.2. *Effects of different control measures*

We proceed to evaluate the effectiveness of various control measures. Our primary recommendation is to enforce mask-wearing among participants, except during lunch breaks. To gauge the efficacy of this measure, we conducted simulations by varying the proportion of participants wearing masks while holding other parameters unchanged. Figure 3(a) illustrates the relationship between the average final size of the epidemic and the mask-wearing compliance rate. Our findings indicate a substantial reduction in the total number of infections as the mask-wearing rate increases. Notably, when 90% of participants wear masks, the average number of infections decreases to 140—a stark contrast to the nearly 210 infections recorded in the absence of mask usage. This result underscores the protective effect of high compliance with mask mandates, effectively minimizing the risk of infection among susceptible individuals and playing a pivotal role in epidemic mitigation.

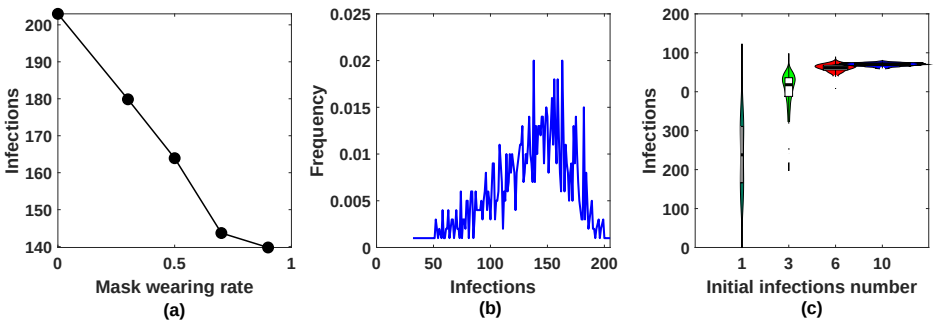

Figure 3. Impact of control measures on epidemic dynamics: (a) varying mask-wearing rates among all participants, (b) mandating masks specifically for initial infections, and (c) reducing the number of initial infections. All results were derived from 1000 independent simulation runs.

A targeted strategy to curb the spread of infectious diseases at conferences involves mandating masks for individuals who are identified as infectious. Through nucleic acid testing (NAT) or symptom screening, participants testing positive can be identified; however, if attendance is unavoidable, requiring these infectious individuals to wear masks is crucial. Figure 3(b) demonstrates that, under this scenario, infection numbers predominantly range from 60 to 200, with the highest density between 100 and 170. Compared to the baseline scenario without interventions, this targeted approach significantly lowers the infection count, confirming its efficacy in curtailing the final epidemic size.

Another fundamental approach involves preventing infected individuals from attending altogether, achievable through rigorous pre-conference screening (e.g., NAT) to reduce the initial number of

infectious seeds. To assess the effectiveness of this exclusion strategy, we varied the number of initial infectious individuals $I_0 \in \{1, 3, 6, 10\}$ while assuming a constant 60% mask-wearing rate among participants. As shown in Figure 3(c), the final epidemic size decreases markedly as the number of initial infections decreases. Specifically, a strong positive correlation exists between the initial infectious seed size and the total number of secondary infections, highlighting the critical importance of entry screening.

3.3. Effects of adjusting the meeting schedule

Our baseline analysis indicated that a significant portion of transmission events occur during rest periods and lunch breaks. Consequently, we explored adjustments to the meeting schedule—specifically, modifying the duration and structure of these high-risk intervals—to minimize infection risk. We first analyzed the impact of shortening rest periods by testing intervals of 10, 15, 20, 25, or 30 minutes. Figure 4(a) reveals that reducing the rest duration from 30 to 15 minutes does not significantly impact the cumulative number of infections. This suggests that simply shortening break times, without altering behavior or contact patterns, may be insufficient to effectively reduce transmission.

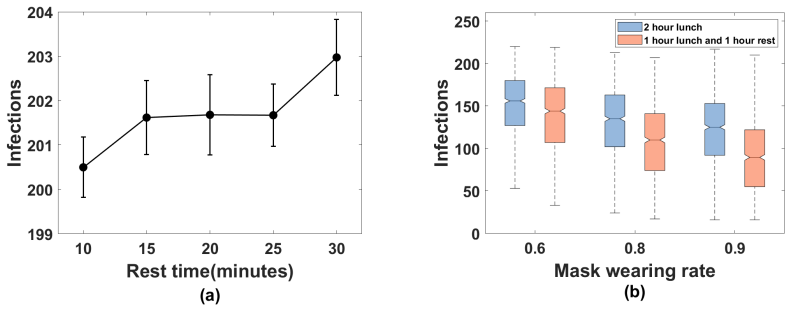

Figure 4. Impact of schedule adjustments on infection numbers: (a) shortening rest periods and (b) restructuring the lunch break. The rest durations explored were 10, 15, 20, 25, and 30 minutes. Restructuring involved splitting a continuous 2-hour lunch into a 1-hour lunch session and a 1-hour rest period, during which mask-wearing was enforced. Results were based on 1000 independent simulation runs.

Further exploration involved restructuring the lunch break to reduce unmasked exposure time. We simulated a scenario where a continuous 2-hour lunch block was divided into a 1-hour lunch session and a 1-hour rest period. The rationale is that participants would wear masks during the designated rest period, unlike during lunch. As depicted in Figure 4(b), the number of infections decreases monotonically as the mask-wearing compliance during the rest period increases. A split schedule (1-hour lunch + 1-hour mask rest) results in significantly fewer infections than a continuous 2-hour lunch period. These outcomes suggest that restructuring unstructured breaks to incorporate masked

intervals can be an effective strategy for epidemic control in conference settings.

3.4. Impact of multiple control measures on epidemic evolution

In the preceding sections, we evaluated the impact of individual prevention and control measures on epidemic dynamics. However, to formulate a robust strategy for epidemic mitigation, it is essential to assess the synergistic effects of combining multiple interventions. Consequently, we conducted a comprehensive analysis integrating participant mask-wearing, schedule adjustments, restroom management, and the reduction of initial infections.

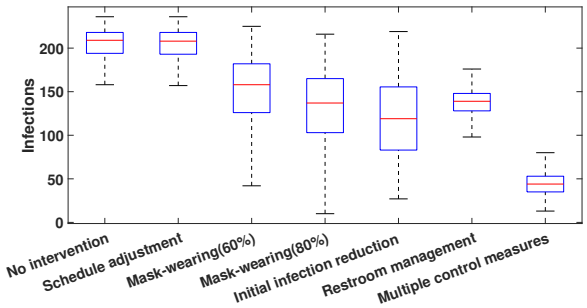

Strategy Type	**Specific Implementation**
Participant mask-wearing	Mask-wearing compliance of 60% or 80% among participants
Schedule adjustment	Splitting the 2-hour lunch break into a 1-hour lunch and a 1-hour rest
Restroom management	Regular disinfection and enhanced ventilation of restrooms
Initial infection reduction	Reduction of the number of initial infectious individuals to 1
Multiple control measures	Integration of participant mask-wearing (60%), schedule adjustments, restroom management, and initial infection reduction

Figure 5. Comparative efficacy of single versus multiple control measures on infection outcomes. Scenarios include no intervention, single interventions (participant mask-wearing at 60% or 80%, schedule adjustments, initial infection reduction, restroom management), and a combination strategy combining multiple measures. Detailed descriptions of each intervention are provided in the table at the bottom. All results were derived from 1000 independent simulation runs.

To compare the efficacy of these measures, Figure 5 shows the final infection counts under three scenarios: no control measures, single control measures, and multiple control measures. The results demonstrate that while implementing any single intervention—such as increasing mask compliance or adjusting the schedule—leads to a reduction in infections compared to the baseline, the most substantial reduction is achieved when these measures are applied in tandem.

From the simulation results in Figure 5, we observe that a multi-faceted approach involving (i) reducing the initial infection seeds to 1, (ii) maintaining a 60% mask-wearing rate, (iii) restructuring the lunch schedule to a 1-hour lunch and a 1-hour rest, and (iv) implementing rigorous restroom disinfection and ventilation can reduce the cumulative infection count from approximately 200 to 50.

This represents a 75% reduction in total infections, highlighting the critical importance of a layered defense strategy.

4. Discussion

Our study presents a comprehensive agent-based model (ABM) designed to simulate the transmission of an infectious disease at the individual level during a one-day conference. By partitioning the conference schedule into distinct activities—such as meetings, rest periods, and lunch breaks—the model effectively captures participants' movement patterns and the potential for rapid infection within a concentrated timeframe. Notably, our framework is parameterized to reflect the transmission dynamics of highly infectious pathogens, specifically the SARS-CoV-2 Omicron variant.

The results underscore the critical importance of implementing multi-layered prevention and control measures to mitigate disease spread in professional gatherings. In the absence of interventions, our simulations yield a mean attack rate of approximately 84%. This finding aligns with documented empirical data from super-spreading events, such as the Skagit Valley Choir outbreak (86.7%) [31] and the Oslo Christmas party outbreak (76%) [32]. Furthermore, our results are consistent with a recent pilot study on COVID-19 mitigation during an in-person conference [33]. While single measures—such as mask mandates, reducing initial infectious seeds, or schedule adjustment—show efficacy, the most substantial reduction in transmission is achieved through their synergistic implementation. By integrating mask-wearing, schedule optimization, and enhanced restroom management (specifically ventilation), the cumulative infection count can be suppressed to a minimal level.

Despite the insights provided, several limitations in the current model warrant acknowledgment. First, we assumed well-mixed dynamics during lunch breaks, modeled as a random work process. This assumption represents standing buffet-style lunches or networking sessions where attendees circulate freely. However, many conferences use fixed seating (e.g., round tables), which can induce local contact clusters and potentially reduce the effective reproduction number compared to the random-mixing scenario.

A key advantage of our proposed ABM is its inherent generalizability. The modular framework allows for the integration of diverse behavioral rules. While this study focuses on a high-mobility buffet scenario to estimate the potential upper-bound transmission risks, the model can be readily extended to simulate fixed-seating patterns by constraining agent mobility to specific spatial zones. Future studies can utilize this framework to quantify the protective efficacy of switching from buffet-style to partitioned seating arrangements.

Furthermore, while this study focuses on a single-day event, the model is extensible to multi-day conferences (e.g., 2–3 days). Such scenarios can be simulated by iterating the model through a sequence of single-day cycles. A central assumption in this extension is the "environmental reset": we posit that, due to overnight ventilation and disinfection, viral concentrations in the air and on surfaces dissipate to zero before the start of each subsequent day. However, the attendees' epidemiological states would propagate through the sessions. Multi-day simulations would need to incorporate the temporal dynamics of viral shedding; for instance, agents in the "Exposed" state on Day 1 may transition to the "Infectious" state on Day 2 or Day 3, depending on the variant-specific incubation period. Future iterations will incorporate these time-dependent viral load trajectories to quantify cumulative risks over the full duration of an international event.

Finally, our model currently assumes homogeneity among agents in terms of viral shedding and susceptibility. In natural settings, transmission is often characterized by significant over-dispersion, where a small fraction of individuals ("super-spreaders") accounts for a disproportionately large number of infections—the so-called 20/80 rule. From a dynamical systems perspective, the presence of even a single super-spreader can drastically accelerate transmission, leading to clustered, explosive outbreaks [34, 35]. While we utilized a uniform viral load to establish a baseline risk assessment, the agent-based framework is fully capable of incorporating biological heterogeneity. Future versions of the model will address this by assigning individual-level parameters drawn from over-dispersed probability distributions (e.g., negative binomial). This extension will better capture the stochastic nature of super-spreading events, which remain critical drivers of outbreaks in confined settings.

In conclusion, the computational model proposed here serves as a valuable quantitative tool for assessing epidemic evolution under varied intervention strategies. By predicting the impact of specific measures across different scenarios, the framework provides actionable insights for both policymakers and conference organizers to minimize transmission risks and build a foundation for future quantitative public health research.

Use of AI tools declaration

The authors declare they have not used Artificial Intelligence (AI) tools in the creation of this article.

Acknowledgments

The authors thank Dr. Xiaopeng Qi from the Chinese Center for Disease Control and Prevention for the helpful discussions.

Conflict of interest

The authors declare there is no conflict of interest.

References

1. World Health Organization, Press conference of WHO-China Joint Mission on COVID-19, 2020. Available from: https://www.who.int/docs/default-source/coronaviruse/who-china-joint-mission-on-covid-19-final-report.pdf.
2. World Health Organization, Report of the WHO-China Joint Mission on Coronavirus Disease 2019, 2020. Available from: https://www.who.int/docs/default-source/coronaviruse/.
3. W. Zhu, X. Tang, Y. Chen, M. Chen, X. Han, Y. Xie, et al., Prediction of SARS-CoV-2 infection case based on the meta-SEIRS model, *Epidemiol. Infect.*, **152** (2024), e144. https://doi.org/10.1017/S0950268824001274
4. B. Tang, X. Wang, Q. Li, N. L. Bragazzi, S. Tang, Y. Xiao, et al., Estimation of the transmission risk of 2019-nCov and its implication for public health interventions, *J. Clin. Med.*, **9** (2020), 462. https://doi.org/10.3390/jcm9020462

5. F. Wilta, A. L. C. Chong, G. Selvachandran, K. Kotacha, W. Ding, Generalized susceptible-exposed-infectious-recovered model and its contributing factors for analysing the death and recovery rates of the COVID-19 pandemic, *Appl. Soft Comput.*, **123** (2022), 108973. https://doi.org/10.1016/j.asoc.2022.108973

6. Y. Yan, Y. Chen, K. Liu, X. Luo, B. Xu, Y. Jiang, et al., Modeling and prediction for the trend of outbreak of NCP based on a time-delay dynamic system (in Chinese), *Sci. Sin. Math.*, **50** (2020), 385–392.

7. Y. Deng, S. Xing, M. Zhu, J. Lei, Impact of insufficient detection in COVID-19 outbreaks, *Math. Biosci. Eng.*, **18** (2021), 9727–9742. https://doi.org/10.3934/mbe.2021476

8. T. Alamo, D. G. Reina, P. M. Gata, V. M. Preciado, G. Giodano, Data-diven methods for presnet and future pandemics: Monitoring, modelling and managing, *Annu. Rev. Control*, **52** (2021), 448–464. https://doi.org/10.1016/j.arcontrol.2021.05.003

9. S. Venkatramanan, B. Lewis, J. Chen, D. Higdon, A. Vullikanti, M. Marathe, Using data-driven agent-based models for forecasting emerging infectious diseases, *Epidemics*, **22** (2018), 43–49. https://doi.org/10.1016/j.epidem.2017.02.010

10. D. Bertsimas, L. Boussioux, R. Cory-Wright, A. Delarue, V. Digalakis, A. Jacquillat, et al., From predictions to prescriptions: A data-driven response to COVID-19, *Health Care Manag. Sci.*, **24** (2021), 253–272. https://doi.org/10.1007/s10729-020-09542-0

11. T. H. Kim, R. Chinthaginjala, A. Srinivasulu, S. P. Tera, S. O. Rab, COVID-19 health data prediction: A critical evaluation of CNN-based approaches, *Sci. Rep.*, **15** (2025), 9121, https://doi.org/10.1038/s41598-025-92464-0

12. M. Ajelli, B. Gonçalves, D. Balcan, V. Colizza, H. Hu, J. J. Ramasco, et al., Comparing large-scale computational approaches to epidemic modeling: Agent-based versus structured metapopulation models, *BMC Infect. Dis.*, **10** (2010), 190. https://doi.org/10.1186/1471-2334-10-190

13. C. Xu, Y. Pei, S. Liu, J. Lei, Effectiveness of non-pharmaceutical interventions against local transmission of COVID-19: An individual-based modelling study, *Infect. Dis. Modell.*, **6** (2021), 848–858. https://doi.org/10.1016/j.idm.2021.06.005

14. S. L. Chang, N. Harding, C. Zachreson, O. M. Cliff, M. Prokopenko, Modelling transmission and control of the COVID-19 pandemic in Australia, *Nat. Commun.*, **11** (2020), 5710. https://doi.org/10.1038/s41467-020-19393-6

15. F. Wu, X. Liang, J. Lei, Modelling COVID-19 epidemic with confirmed cases-driven contact tracing quarantine, *Infect. Dis. Modell.*, **8** (2023), 415–426. https://doi.org/10.1016/j.idm.2023.04.001

16. X. Weng, Q. Chen, T. K. Sathapathi, X. Yin, L. Wang, Impact of school operating scenarios on COVID-19 transmission under vaccination in the U.S.: An agent-based simulation model, *Sci. Rep.*, **13** (2023), 12836, https://doi.org/10.1038/s41598-023-37980-7

17. G. Brida, N. Garrido, An agent-based and microsimulated model of the epidemiology impact of closure of schools during the COVID-19 pandemic in the region of Aysen in Chile, *J. Dyn. Games*, **10** (2023), 255–269. https://doi.org/10.3934/jdg.2023003

18. F. Pilati, A. Sbaragli, M. Nardello, L. Santoro, D. Fontanelli, D. Brunelli, Indoor positioning systems to prevent the COVID19 transmission in manufacturing environments, *Procedia CIRP*, **107** (2022), 1588–1593. https://doi.org/10.1016/j.procir.2022.05.195

19. Q. Qiao, C. Cheung, A. Yunusa-Kaltungo, P. Manu, R. Cao, Z. Yuan, An interactive agent-based mdoelling framework for assessing COVID-19 transmission risk on construction site, *Saf. Sci.*, **168** (2023), 106312. https://doi.org/10.1016/j.ssci.2023.106312

20. L. López, L. Giovanini, Adaptive dynamic social networks using an agent-based model to study the role of social awareness in infectious disease spread, *Physica D: Nonlinear Phenom.*, **472** (2025), 134530. https://doi.org/10.1016/j.physd.2025.134530

21. D. Kerkmann, S. Korf, K. Nguyen, D. Abele, A. Schengen, C. Gerstein, et al., Agent-based modeling for realistic reproduction of human mobility and contact behavior to evaluate test and isolation strategies in epidemic infectious disease spread, *Comput. Biol. Med.*, **193** (2025), 110269. https://doi.org/10.1016/j.compbiomed.2025.110269

22. M. K. Chae, D. U. Hwang, K. Nah, W. S. Son, Evaluation of COVID-19 intervention policies in South Korea using the stochastic individual-based model, *Sci. Rep.*, **13** (2023), 18945. https://doi.org/10.1038/s41598-023-46277-8

23. A. Rodríguez, E. Cuevas, D. Zaldivar, B. Mordales-Castañeda, R. Sarkar, E. H. Houssein, An agent-based transmission model of COVID-19 for reopening policy design, *Comput. Biol. Med.*, **148** (2022), 105847. https://doi.org/10.1016/j.compbiomed.2022.105847

24. Y. Deng, M. Li, J. Lei, Evaluation of infectious diseases control using an individual model under the test-trace-isolate program, *Med. Res. Arch.*, **12** (2024), 11. https://doi.org/10.18103/mra.v12i11.5987

25. D. K. Chu, E. A. Akl, S. Duda, K. Solo, S. Yaacoub, H. J. Schünemann, Physical distancing, face masks, and eye protection to prevent person-to-person transmission of SARS-CoV-2 and COVID-19: A systematic review and meta-analysis, *Lancet*, **395** (2020), 1973–1987. https://doi.org/10.1016/S0140-6736(20)31142-9

26. K. L. Andrejko, J. M. Pry, J. F. Myers, N. Fukui, J. L. DeGuzman, J. Openshaw, et al., Effectiveness of face mask of respirator use in indoor public settings for prevention of SARS-Cov-2 infection—California, Feburaury–December 2021, *MMWR Morb Mortal Wkly Rep.*, **71** (2022), 212–216. https://doi.org/10.15585/mmwr.mm7106e1

27. J. Howard, A. Huang, Z. Li, Z. Tufekci, V. Zdimal, H. M. van der Westhuizen, et al., An evidence review of face masks against COVID-19, *Proc. Natl. Acad. Sci. USA*, **118** (2021), e2014564118. https://doi.org/10.1073/pnas.2014564118

28. J. Lai, K. K. Coleman, S. H. S. Tai, J. German, F. Hong, B. Albert, et al., Relative efficacy of masks and respirators as source control for viral aerosol shedding from people infected with SARS-CoV-2: A controlled human exhaled breath aerosol experimental study, *EBioMedicine*, **104** (2024), 105157. https://doi.org/10.1016/j.ebiom.2024.105157

29. N. A. Khan, H. Al-Thani, A. El-Menyar, The emergence of new SARS-CoV-2 variant (Omicron) and increasing calls for COVID-19 vacine boosters-The debate continues, *Travel Med. Infect. Dis.*, **45** (2022), 102246. https://doi.org/10.1016/j.tmaid.2021.102246

30. K. Sun, S. Tempia, J. Kleynhans, A. von Gottberg, M. L. McMorrow, N. Wolter, et al., SARS-CoV-2 transmission, persistence of immunity, and estimates of Omicron's impact in South African population cohorts, *Sci. Transl. Med.*, **14** (2022), eabo7081. https://www.science.org/doi/abs/10.1126/scitranslmed.abo7081

31. L. Hamner, P. Dubbel, I. Capron, A. Ross, A. Jordan, J. Lee, et al., High SRAS-CoV-2 attack rate following exposure at a choir practice—Skagit County, Washington, March 2020, *MMWR Morb Mortal Wkly Rep.*, **69** (2020), 606–610. https://doi.org/10.15585/mmwr.mm6919e6

32. L. T. Brandal, E. MacDonald, L. Veneti, T. Ravlo, H. Lange, U. Naseer, et al., Outbreak caused by SARS-CoV-2 Omicron variant in Norway, November to December 2021, *Eurosurveillance*, **26** (2021), 2101147. https://doi.org/10.2807/1560-7917.ES.2021.26.50.2101147

33. L. Servitje, T. McAndrew, K. Bachynski, C. Cronin, M. Lincoln, J. K. Marsh, et al., Can a conference be epidemiologically conscious? A pilot study of implementing COVID-19 mitigation measures at an in-person conference, *medRxiv*. https://doi.org/10.1101/2025.06.30.25328802

34. K. Sneppen, R. J. Taylor, L. Simonsen, Impact of superspreaders on dissemination and mitigation of COVID-19, *medRxiv*. https://doi.org/10.1101/2020.05.17.20104745

35. K. Sneppen, B. F. Nielsen, R. J. Taylor, L. Simonsen, Overdispersion in COVID-19 increases the effectiveness of limiting nonrepetitive contacts for transmission control, *Proc. Natl. Acad. Sci. USA*, **118** (2021), e2016623118. https://doi.org/10.1073/pnas.2016623118

Appendix

A. Parameters of the random walk

Table A1 lists the parameters used to simulate the random walk of individuals.

Table A1. Parameters of the random walk.

Parameter	Description	Value[(a)]	Unit
CR	the conversation rate of two individuals	uniform(0, 1)	s^{-1}
TR	upper limit of the conversation rate of two individuals	0.075	s^{-1}
NR	movement probability of individual	uniform(0, 1)	s^{-1}
MR	upper limit of the movement probability	0.175	s^{-1}
talklimit	upper limit of individual conversation time	Gamma(*ta*, *tb*)	s
ta	a parameter of limited conversation time	80	s
tb	another parameter of limited conversation time	6	s
cd	close conversation distance	0.5	m
cdm	close contact distance	2	m
sa	the abscissa of the initial coordinate position	2	m
sb	the ordinate of the initial coordinate position	2	m

[(a)] uniform(0, 1) means a random number with uniform distribution in [0, 1], Gamma(*ta*, *tb*) means a gamma distribution random number with parameter *ta* and *tb*.

B. Timing of the next visit to the restroom

The function $p(a;t)$ represents the probability density such that $p(a;t)\Delta a$ denotes the probability of a participant utilizing the restroom during the time interval $(t+a, t+a+\Delta a)$ from the first time, commencing from the current time t. The function $q(a;t)$ denotes the likelihood of a participant refraining from using the restroom between the current time t and $t+a$, and $f(a;t)$ represents the density function such that $f(a;t)\Delta a$ indicates the probability of a participant utilizing the restroom during the time interval $(t+a, t+a+\Delta a)$. We have

$$\begin{aligned} p(a;t) &= C(t)^{-1} f(a;t) q(a;t), \\ C(t) &= \int_0^{+\infty} f(a;t) q(a;t) \mathrm{d}a. \end{aligned} \tag{B.1}$$

B.1. The function $q(a;t)$ and $f(a;t)$

To estimate the functions $q(a;t)$ and $f(a;t)$, we introduce the following assumptions:

(1) Each participant typically visits the restroom with a uniform frequency f_0, implying that the probability of a restroom visit within a short time interval Δt is $f_0 \Delta t$.
(2) The conference schedule time points (depicted in Figure B1) are denoted as

$$T = (T_0, T_1, T_2, \cdots, T_{2n}),$$

where T_0 signifies the commencement of the conference, the intervals $[T_{2k}, T_{2k+1}]$ represent rest or lunch breaks, and $[T_{2k+1}, T_{2(k+1)}]$ signify meeting periods. Participants do not visit the restroom during meetings.
(3) All participants depart from the conference venue at T_{2n}.
(4) Participant restroom visits are independent events.

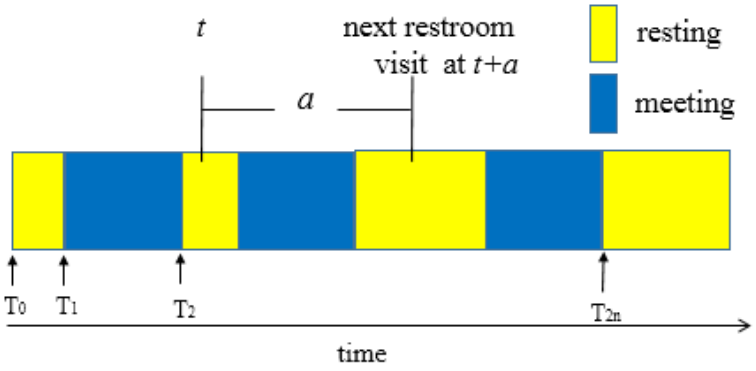

Figure B1. Estimating the timing of restroom usage.

First, we assume that participants are currently in a break period $t \in [T_{2k}, T_{2k+1}]$, disregarding scheduled meetings and allowing participants to use the restroom at their convenience. Consequently, we have

$$q(a;t) = e^{-f_0 a}. \tag{B.2}$$

Now, we account for the meeting schedule's impact.

It the time point $t+a$ falls within the resting interval $[T_{2k}, T_{2k+1}]$, i.e., $0 < a < T_{2k+1} - t$, we maintain

$$q(a;t) = e^{-f_0 a}. \tag{B.3}$$

When the time point $t + a$ aligns with the meeting period, i.e., $t + a \in [T_{2j+1}, T_{2(j+1)}]$, or $a \in [T_{2j+1} - t, T_{2(j+1)} - t]$ $(j \geq k)$, participants abstain from restroom visits during meetings. Therefore,

$$q(a;t) = q(T_{2j+1} - t; t). \tag{B.4}$$

If the time point $t+a$ coincides with the resting period, i.e., $t+a \in [T_{2j}, T_{2j+1}]$ $(j \geq k+1)$, participants may exhibit a heightened need for a restroom visit due to lack of access during meetings. Let $\hat{f}_j$ denote the adjusted restroom visit frequency during $t + a \in [T_{2j}, T_{2j+1}]$. Noting that $q(a;t)|_{a=T_{2j}-t} = q(T_{2j-1} - t; t)$, we express

$$q(a;t) = q(T_{2j-1} - t; t)e^{-\hat{f}_j(a+t-T_{2j})}, \quad a \in [T_{2j} - t, T_{2j+1} - t]. \tag{B.5}$$

The adjusted frequency $\hat{f}_j$ can be determined by assuming that participants have the same probability of not using the restroom during $[t, t+T_{2j+1}]$ as they would in the absence of meetings. Hence, comparing (B.2) with (B.5), we derive

$$e^{-f_0(T_{2j+1}-t)} = q(T_{2j-1}; t)e^{-\hat{f}_j(T_{2j+1}-T_{2j})},$$

yielding

$$\hat{f}_j = \frac{f_0(T_{2j+1} - t) + \ln q(T_{2j-1} - t; t)}{T_{2j+1} - T_{2j}}.$$

Moreover, following the frequency adjustment, the probability $q(T_{2j-1} - t; t)$ equates to that without meetings, i.e.,

$$q(T_{2j-1} - t; t) = e^{-f_0(T_{2j-1}-t)}.$$

Thus, the adjusted frequency becomes

$$\hat{f}_j = \frac{T_{2j+1} - T_{2j-1}}{T_{2j+1} - T_{2j}} f_0, \tag{B.6}$$

resulting in

$$q(a;t) = e^{-f_0(T_{2j-1}-t)+\hat{f}_j(T_{2j}-t)}e^{-\hat{f}_j a}. \tag{B.7}$$

In summary, we obtain (where $t \in (T_{2k}, T_{2k+1})$)

$$q(a;t) = \begin{cases} e^{-f_0 a}, & t < a + t \leq T_{2k+1} \\ e^{-f_0(T_{2j+1}-t)}, & T_{2j+1} \leq a + t \leq T_{2(j+1)},\ j \geq k \\ e^{-f_0(T_{2j-1}-t)+\hat{f}_j(T_{2j}-t)}e^{-\hat{f}_j a}, & t_{2j} \leq a + t \leq T_{2j+1},\ j \geq k+1. \end{cases}$$

Here, $T_{2n+1} = +\infty$, thus $\hat{f}_n = f_0$.

Let $f(a;t)\Delta a$ represent the probability of a participant using the restroom during the time interval $(t + a, t + a + \Delta a)$, then

$$f(a;t) = \begin{cases} f_0, & t < a + t \leq T_{2k+1} \\ 0, & T_{2j+1} \leq a + t \leq T_{2(j+1)},\ j \geq k \\ \hat{f}_j, & T_{2j} \leq a + t \leq T_{2j+1},\ j \geq k+1. \end{cases}$$

B.2. The function $p(a;t)$

Now, let's evaluate $C(t)$, which is given by

$$\begin{aligned} C(t) &= \int_0^{+\infty} f(a;t)q(a;t)\mathrm{d}a \\ &= \int_0^{T_{2k+1}-t} f_0 e^{-f_0 a}\mathrm{d}a + \sum_{j=k+1}^{n-1}\int_{T_{2j}-t}^{T_{2j+1}-t} \hat{f}_j e^{-f_0(T_{2j-1}-t)+\hat{f}_j(T_{2j}-t)}e^{-\hat{f}_j a}\mathrm{d}a \\ &\quad + \int_{T_{2n}-t}^{+\infty} \hat{f}_n e^{-f_0(T_{2n-1}-t)+\hat{f}_n(T_{2n}-t)}e^{-\hat{f}_n a}\mathrm{d}a \\ &= 1 - e^{-f_0(T_{2k+1}-t)} + \sum_{j=k+1}^{n-1} e^{-f_0(T_{2j-1}-t)}\left(1 - e^{-\hat{f}_j(T_{2j+1}-T_{2j})}\right) + e^{-f_0(T_{2n-1}-t)}. \end{aligned}$$

The probability $p(a;t)$ is then given by

$$\begin{aligned} p(a;t) &= C(t)^{-1} f(a;t)q(a;t) \\ &= C(t)^{-1} \times \begin{cases} f_0 e^{-f_0 a}, & t < a + t \le T_{2k+1} \\ 0, & T_{2j+1} \le a + t \le T_{2(j+1)},\ j \ge k \\ \hat{f}_j e^{-f_0(T_{2j-1}-t)+\hat{f}_j(T_{2j}-t)}e^{-\hat{f}_j a}, & T_{2j} \le a + t \le T_{2j+1},\ j \ge k+1. \end{cases} \end{aligned}$$

B.3. The function $F(a;t)$ and the numerical scheme to determine the next time to visit the restroom

To calculate the time interval that a participant uses the restroom, we utilize the distribution function $F(a;t)$, defined as

$$F(a;t) = \int_0^a p(a';t)\mathrm{d}a'.$$

The graph of the function $F(a;t)$ is shown in Figure B2. By employing $F(a;t)$ along with a uniform random number s in the interval $[0, 1]$, we solve the equation $s = F(a;t)$ to determine the time a for a participant at the current moment t. The next visit to the restroom is scheduled at $t + a$.

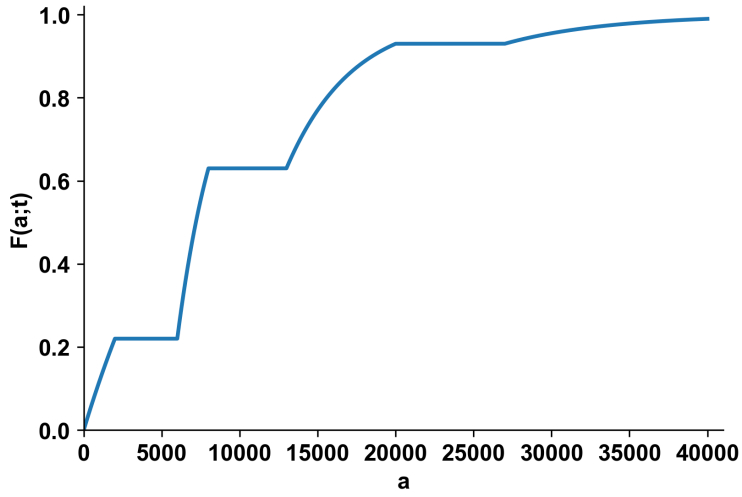

Figure B2. Plot of the function $F(a;t)$.

Let's define

$$\varphi_i(a,t) = \begin{cases} 1 - e^{-f_0 a}, & i = k \\ e^{-f_0(T_{2i-1}-t)}(1 - e^{\hat{f}_i(a+t-T_{2i})}), & k < i \le n \end{cases}$$

Then, $C(t)$ can be expressed as (we note $t_{2n+1} = \infty$)

$$C(t) = \sum_{i=k}^{n} \varphi_i(T_{2i+1} - t; t).$$

A detailed calculation leads to:

$$F(a;t) = \begin{cases} C(t)^{-1}\varphi_k(a;t), & 0 \le a < T_{2k+1} - t, \\ C(t)^{-1}\sum_{i=k}^{j} \varphi_i(T_{2i+1} - t; t), & T_{2k+1} - t \le a < T_{2(k+1)} - t, \\ C(t)^{-1}\left(\sum_{i=k}^{j-1} \varphi_i(T_{2i+1} - t; t) + \varphi_j(a;t)\right), & T_{2j} - t \le a < T_{2j+1} - t \ (k+1 \le j \le n). \end{cases}$$

Here is a numerical scheme to determine when a participant should next use the restroom, based on the current time t:

Input: The current time t, the schedule $\{T_i\}$

Output: The time of the next restroom visit $t + a$.

(1) Find the value of k such that $T_{2k} < t < T_{2k+1}$.

(2) Calculate $A_i = \varphi_i(T_{2i+1} - t; t), (i = k, k+1, \ldots, n)$.

(3) Calculate

$$C = \sum_{i=k}^{n} A_i.$$

(4) Generate a uniform random number $s \in [0, 1]$.

(5) Find the value of j such that $k \le j \le n$ and

$$\frac{1}{C}\sum_{i=k}^{j-1} A_i < s < \frac{1}{C(t)}\sum_{i=k}^{j} A_i,$$

then calculate

$$s_0 = s - \frac{1}{C}\sum_{i=k}^{j-1} A_i$$

(6) Solve the equation

$$\varphi_j(a;t) = s_0$$

for a, and the time of the next restroom visit is given by $t + a$. Explicitly,

$$t + a = \begin{cases} t - {f_0}^{-1}\ln(1 - s_0), & j = k, \\ T_{2j} - \hat{f}_j^{-1}\ln(1 - s_0 e^{f_0(T_{2j-1}-t)}), & j > k. \end{cases} \tag{B.8}$$

Utilizing the above numerical scheme, we can approximate the timing of restroom usage for each participant based on their designated schedule $\{T_i\}$.

C. Environmental infection rate in the restroom

Here, we calculate the dynamics of environmental viral load in the restroom during the conference and subsequently estimate the environmental infection rate. Initially, our focus lies on assessing virus transmission within the restroom environment. Consequently, we primarily consider the dynamics of viral load, accounting for both increases and decreases driven by routine ventilation and disinfection procedures. Moreover, individuals using the restroom must be categorized as either infectious or susceptible. If deemed infectious, the total viral load in the environment at that time must be calculated. Conversely, for susceptible individuals, the environmental infection rate needs to be determined.

Subsequently, we delve into the transmission of the virus from contaminated objects to individuals. We presume that infectious individuals contaminate the environment through touch and droplets upon entering the restroom, posing a risk of infection to susceptible individuals who come into contact with contaminated surfaces. The infection risk for the susceptible is influenced by factors such as vaccination status and hand hygiene practices. Notably, we assume that transmission via touch is primarily through direct contact rather than airborne transmission, thus rendering mask-wearing rates irrelevant in this context.

First, we introduce several key notations used in our derivation:

- V: The volume of the restroom.
- $X(t)$: The virus load of the restroom at the current moment. Initially, $X_0 = 0$. The viral load increases as infectious individuals enter the restroom and decreases due to regular ventilation and disinfection.
- α: The rate at which infectious individuals release the virus.
- $b(t)$: The reduction rate of virus at time t.
- $\beta_i(t)$: The environmental infection rate of susceptible i in the restroom from time t, so that $\beta_i(t)\Delta t$ indicates the probability that susceptible i was not infected before time t but was infected within $[t, t + \Delta t]$.
- $\beta_{\max}$: The maximum infection rate of the virus to individuals.
- $\beta_{\max(i)}$: The maximum infection rate of the virus to individual i.
- S_0: The basic infection rate of infected objects to individuals in the restroom (including door handles, stalls, and sinks).
- $d(t)$: Indicates whether the restroom door handle of the restroom is infected.
- $h_j(t)$: Indicates whether the jth stall in the restroom is infected.
- μ_i: The probability that susceptible individual i in the restroom is infected by infected objects.
- PW: The probability that individuals go to the restroom and wash their hands.
- G_i: The protective effect of virus release load of infectious individual i of wearing a mask:

$$G_i = \begin{cases} 1, & \text{if } i \text{ is unmasked,} \\ 0.11, & \text{if } i \text{ is masked.} \end{cases} \tag{C.1}$$

- K_i: The infection risk of susceptible individual i when wearing a mask:

$$K_i = \begin{cases} 1, & \text{if } i \text{ is unmasked,} \\ 0.33, & \text{if } i \text{ is masked.} \end{cases} \tag{C.2}$$

- V_i: The impact factor of vaccine for susceptible individuals:

$$V_i = \begin{cases} 0, & \text{if } i \text{ is not vaccinated,} \\ 0.3, & \text{if } i \text{ is vaccinated or recovered.} \end{cases} \tag{C.3}$$

- ε_i: Indicates whether individual i enters the restroom at time t:

$$\varepsilon_i(t) = \begin{cases} 1, & \text{if } i \text{ is in the restroom,} \\ 0, & \text{otherwise.} \end{cases} \tag{C.4}$$

For each object in the restroom, a status variable indicates its infection status. When the infection enters the restroom and comes into contact with the object, if the object's infection status becomes 1, it means the object is infected. The infection status of all objects changes to 0 after the next disinfection cycle. To implement this, we assign a corresponding infection state variable for each object (including the door, each stall in the restroom, and each sink). Then, based on the contact between the object and the infectious individual, we set the infection state variable accordingly.

Using this process, we can determine the infection situation $d(t)$ of the door handle and the infection situation $h_j(t)$ for the jth stall in the restroom. The corresponding expressions for these are as follows: the infection situation of the door handle $d(t)$ is defined as:

$$d(t) = \begin{cases} 1, & \text{if the handle is infected, } T_0 < t < T_1, \text{ where } T_0 \text{ is the time of the first infectious} \\ & \text{individuals entering the restroom (assuming the individual will definitely touch} \\ & \text{the door), } T_1 \text{ is the time of the first disinfection from } T_0, \\ 0, & \text{if the door is not infected, at other times.} \end{cases}$$

For restrooms without a restroom door, we $d(t) = 0$ for simplicity. The infection status of the jth stall $h_j(t)$ is expressed as:

$$h_j(t) = \begin{cases} 1, & \text{the } j\text{th stall is infected, } T_{0,j} < t < T_1, \text{ where } T_0 \text{ is the time when the infectious} \\ & \text{individuals first enter the } j\text{th stall, } T_1 \text{ is the first disinfection time from } T_0, \\ 0, & \text{if the } j\text{th stall is not infected, at other times.} \end{cases}$$

We do not consider the sink's infection here, assuming hand washing can effectively eliminate virus transmission. However, in practice, individuals may become infected through sinks, albeit with low probability.

It is important to note that a single mathematical formula does not easily describe the dynamics of infection status. In practical calculations, the infection status of each object should be determined based on the specific calculation process rather than relying solely on mathematical formulas.

Next, let's examine the probability μ_i that a susceptible individual is infected by contaminated objects in the restroom. Suppose individuals enter the restroom at time t_0 and stay there for a duration of s. We assume the order of object contact is: restroom door $\rightarrow$ stall $j \rightarrow$ restroom door $\rightarrow$ sink. Then, individuals come into contact with the restroom door and the stall at $t = t_0$, and with the restroom door and the sink at $t = t_0 + s$.

Let w_i indicate whether individual i washes hands. Individual i washes hands with probability PW and does not wash hands with probability $1 - PW$. Based on our assumptions, if the basic infection rate

of object contact is S_0, the probability of individual i becoming infected after contact with the door at time t is:

$$S_0 d(t)(1 - V_i).$$

Therefore, the probability of individual i remaining uninfected after contact with the door is:

$$1 - S_0 d(t)(1 - V_i).$$

Similarly, the probability of individual i remaining uninfected after contacting the stall j at time t is:

$$1 - S_0 h_j(t)(1 - V_i).$$

Considering these situations, the probability that individual i remains uninfected after contacting the outside door and the stall j at time t_0, and remains uninfected after contacting the restroom door at time $t_0 + s$ is:

$$(1 - S_0 d(t_0)(1 - V_i)) \times \left(1 - S_0 h_j(t_0)(1 - V_i)\right) \times (1 - S_0 d(t_0 + s)(1 - V_i)) .$$

The probability of individual i becoming infected is then:

$$1 - \left((1 - S_0 d(t_0)(1 - V_i)) \times \left(1 - S_0 h_j(t_0)(1 - V_i)\right) \times (1 - S_0 d(t_0 + s)(1 - V_i))\right).$$

Considering whether individuals wash their hands, the final comprehensive infection probability is:

$$\mu_i(t_0, s) = (1 - w_i)\left[1 - \left((1 - S_0 d(t_0)(1 - V_i))\left(1 - S_0 h_j(t_0)(1 - V_i)\right)(1 - S_0 d(t_0 + s)(1 - V_i))\right)\right]. \quad \text{(C.5)}$$

Equation (C.5) provides the infection probability of individual i. However, it's important to emphasize that the infection rate should not be solely calculated using this formula in practical calculations. Instead, the infection situation should be determined by simulating an individual using the restroom.

D. The infection rate of individuals after using the restroom

The following method outlines the calculation of the probability that each individual will be infected after using the restroom during a rest period. The primary approach is to compute the probability that individuals remain uninfected after using the restroom, then deduce the probability that they become infected. In our model, we neglect scenarios involving individuals conversing in the restroom. Consequently, there are two primary pathways by which susceptible individuals may become infected in the restroom: direct exposure to environmental viruses and indirect contact with contaminated objects. Therefore, the probability of an individual contracting an infection in the restroom depends on factors such as the viral concentration in the environment, the duration of the individual's visit, and the likelihood of contact with contaminated surfaces.

Assuming an individual i enters the restroom at time t_0, we compute the probability of that individual becoming infected during their stay in the restroom for a duration of s.

We denote:

- $p_i(t_0, s)$: Probability of individual i being infected from entering the restroom at time t_0 until time $t_0 + s$ (refer to Figure D1).
- $q_i(t_0, s)$: Probability of individual i remaining uninfected during the time from entering the restroom at t_0 until $t_0 + s$.

- $\beta_i(t_0 + s)\Delta s$: Probability of individual i being infected within the time interval $[t_0 + s, \Delta s]$.

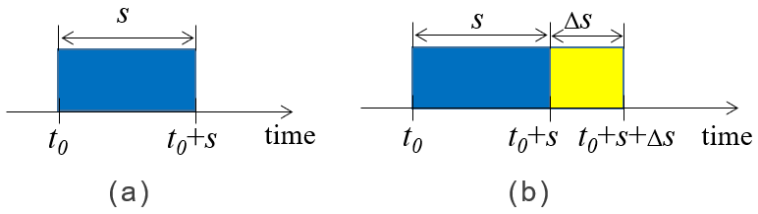

Figure D1. (a) Schematic of $p_i(t_0, s)$. (b) Schematic of $q_i(t_0, s + \Delta s)$.

By definition, $q_i(t_0, s + \Delta s)$ represents the probability of individual i remaining uninfected after a duration $s + \Delta s$ from t_0. It can be segmented into two parts using the multiplication rule of probability: $q_i(t_0, s)$, the probability that individual i remains uninfected after a duration s, multiplied by $q_i(t_0 + s, \Delta s)$, the probability that individual i remains uninfected in the subsequent Δs. This process is illustrated in Figure D1. Thus

$$\begin{aligned} q_i(t_0, s + \Delta s) &= q_i(t_0, s)q_i(t_0 + s, \Delta s) \\ &= q_i(t_0, s)(1 - \beta_i(t_0 + s)\Delta s) \\ &= q_i(t_0, s) - \beta_i(t_0 + s)q_i(t_0, s)\Delta s. \end{aligned} \tag{D.1}$$

Organizing the above equation, we derive

$$\begin{aligned} q_i(t_0, s + \Delta s) - q_i(t_0, s) &= -\beta_i(t_0 + s)q_i(t_0, s)\Delta s \\ \lim_{\Delta s \to 0} \frac{q_i(t_0, s + \Delta s) - q_i(t_0, s)}{\Delta s} &= -\beta_i(t_0 + s)q_i(t_0, s) \\ \frac{\partial q_i(t_0, s)}{\partial s} &= -\beta_i(t_0 + s)q_i(t_0, s). \end{aligned}$$

Given that $q_i(t_0, 0) = 1$ (indicating individual i is uninfected upon entering the restroom), we obtain the differential equation

$$\frac{\partial q_i(t_0, s)}{\partial s} = -\beta_i(t_0 + s)q_i(t_0, s), \quad q_i(t_0, 0) = 1.$$

Solving this differential equation (with t_0 as a parameter), we find

$$q_i(t_0, s) = \exp\left(-\int_0^s \beta_i(t_0 + s')ds'\right).$$

Hence, the probability of individual i being infected within s after entering the restroom is

$$p_i(t_0, s) = 1 - q_i(t_0, s) = 1 - \exp\left(-\int_0^s \beta_i(t_0 + s')ds'\right).$$

In other words,

$$p_i(t_0, s) = 1 - \exp\left(-\int_{t_0}^{t_0+s} \beta_i(s')ds'\right). \tag{D.2}$$

Using the previously calculated $\beta_i(t)$,

$$\beta_i(t) = \beta_{\max(i)}(t)K_i(1 - V_i), \tag{D.3}$$

we have

$$\beta_i(t_0 + s) = \beta_{\max(i)}(t_0 + s)K_i(1 - V_i),$$

where $\beta_{\max(i)}(t_0 + s)$ is defined by

$$\beta_{\max(i)}(t) = \beta_{\max}\frac{(X(t)/X_0)^4}{1 + (X(t)/X_0)^4}. \tag{D.4}$$

Additionally, we must consider situations where susceptible individuals are infected by objects in the restroom. Assuming a susceptible individual enters the restroom at t_0 and stays for a duration s, the time interval during which they are in the restroom is $(t_0, t_0 + s)$. Using the comprehensive infection probability $\mu_i(t_0, s)$ derived previously, the probability of susceptible individual i remaining uninfected can be calculated as

$$1 - \mu_i(t_0, s).$$

Thus, the probability of susceptible individual i remaining uninfected in the restroom after entering at t_0 and staying for s is

$$q_i(t_0, s)(1 - \mu_i(t_0, s)).$$

Consequently, the infection rate of individual i is

$$p_i(t_0, s) = 1 - \left(\exp\left(-\int_{t_0}^{t_0+s} \beta_i(s')ds'\right) \times (1 - \mu_i(t_0, s))\right). \tag{D.5}$$

Ultimately, if an individual contaminates objects in the restroom or becomes infected by them after entering, relying solely on a formula to compute the infection rate might lead to logical confusion. Hence, we recommend simulating this process based on each individual's entry into the restroom rather than relying solely on formulaic calculations. By simulating the process, the actual infection rate can be accurately determined. The steps and implementation details for simulating this process can be elucidated from the formula derivation outlined above.

AIMS Press